



Graphene Field-Effect Transistors for Millimeter Wave Amplifiers

Downloaded from: <https://research.chalmers.se>, 2026-04-04 21:27 UTC

Citation for the original published paper (version of record):

Vorobiev, A., Bonmann, M., Asad, M. et al (2019). Graphene Field-Effect Transistors for Millimeter Wave Amplifiers. International Conference on Infrared, Millimeter, and Terahertz Waves, IRMMW-THz, 2019-September. <http://dx.doi.org/10.1109/IRMMW-THz.2019.8874149>

N.B. When citing this work, cite the original published paper.

Graphene Field-Effect Transistors for Millimeter Wave Amplifiers

A. Vorobiev¹, M. Bonmann¹, M. Asad¹, X. Yang¹, J. Stake¹,
L. Banszerus², C. Stampfer², M. Otto³, and D. Neumaier³

¹Chalmers University of Technology, SE-412 96 Gothenburg, Sweden

²2nd Institute of Physics, RWTH Aachen University, Aachen, 52074 Germany

³Advanced Microelectronic Center Aachen, AMO GmbH, Aachen, 52074 Germany

Abstract— In this work, we analyze high frequency performance of graphene field-effect transistors (GFETs), applying models of drain resistance, carrier velocity and saturation velocity. This allows us to identify main limitations and propose an approach most promising for further development of the GFETs suitable for advanced mm-wave amplifiers. Analysis indicates, that the saturation velocity of charge carriers in the GFETs can be increased up to $5 \cdot 10^7$ cm/s via encapsulating graphene by hexagonal boron nitride layers, with corresponding increase of extrinsic maximum frequency of oscillation up to 180 GHz at 200 nm gate length.

I. INTRODUCTION

OWING to extremely high intrinsic carrier mobility, up to 100 000 cm²/Vs at room temperature, graphene is considered as a promising new channel material in field-effect transistors for advanced mm-wave amplifiers. However, the high frequency performance of the graphene field-effect transistors (GFETs) is limited by a number of intrinsic and extrinsic factors. In particular, the zero-bandgap phenomenon in monolayer graphene results in relatively high drain conductance, which limits the maximum frequency of oscillation (f_{\max}) of the GFETs [1]. Bandgap engineering in graphene is not promising because of simultaneous reduction in the carrier mobility [1]. In this work, we analyze high frequency performance of the GFETs with the high f_{\max} applying models of drain resistance, carrier velocity and saturation velocity. Analysis allows us to identify main limitations and propose most promising approach for further development of the GFETs suitable for mm-wave amplifiers. We show that proper selection of the adjacent dielectric materials with relatively high optical phonon energy can allow for significant increase in the saturation velocity and, hence, f_{\max} of the GFETs.

II. RESULTS

The GFETs have been fabricated in the two-finger gate configuration using high quality, chemical vapor deposited, graphene on oxidized high resistive Si substrates [2]. The technology allows for protection of the top graphene/dielectric interface and, hence, relatively high mobility, up to 2000 cm²/Vs and extremely low contact resistivity, below 100 $\Omega \cdot \mu\text{m}$. This allows for the GFETs operating in the saturation velocity (v_{sat}) mode, up to $v_{\text{sat}} \approx 2 \cdot 10^7$ cm/s, at intrinsic drain field above 1.5 V/ μm . Fig. 1 shows the measured (extrinsic) f_{\max} of the GFETs analyzed in this work together with that of the best previously published GFETs and Si MOSFETs at similar gate lengths (L_g), for comparison [2]. It can be seen, that GFETs in this work reveal record high values of f_{\max} , which are comparable with those of the best reported Si MOSFETs. The lines are simulations using the drain resistance, carrier velocity and saturation velocity models as follows [2,3].

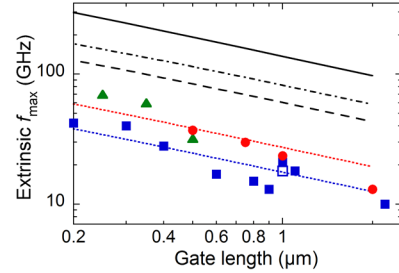


Fig. 1. Extrinsic maximum frequency of oscillation (f_{\max}) versus gate length of GFETs analyzed in this work (circles) shown together with the highest previously published extrinsic f_{\max} of GFETs (squares) and Si MOSFETs (triangles) [2]. The lines are simulations using the models presented in this work. The upper and lower dotted lines correspond to parameters of the GFETs with highest measured f_{\max} (circle) and our previously published GFET (open square), respectively [2,10]. The solid line represents f_{\max} of the GFETs similar to those analyzed in this work, but assuming $g_{\text{ds}}=0.01$ mS, typical for the Si MOSFETs [4]. The dashed and dash-dotted lines represent f_{\max} of the GFETs, similar to these analyzed in this work, but assuming graphene encapsulated by Al₂O₃ and hBN layers, respectively.

Analytical approximation for the extrinsic f_{\max} derived from the GFET small-signal equivalent circuit is [1]

$$f_{\max} = \frac{g_m}{4\pi C_{\text{gs}}} \sqrt{\frac{1}{g_{\text{ds}}(R_i + R_s + R_g) + g_m R_g \frac{C_{\text{gd}}}{C_{\text{gs}}}}}, \quad (1)$$

where g_m and g_{ds} are the intrinsic transconductance and drain conductance, respectively; C_{gs} , and C_{gd} are the gate-source and gate-drain capacitances, respectively; R_g , R_s , and R_i are the gate resistance, source series resistance, and charging resistance of the gate-source capacitance, respectively. We estimated the capacitances as $C_{\text{gs}}=0.5C_{\text{ox}}L_gW_g$ and $C_{\text{gd}}=kC_{\text{gs}}$, where $C_{\text{ox}}=3 \cdot \text{fF} \cdot \mu\text{m}^{-2}$ is the gate oxide capacitance per unit area, W_g is the gate width and k is the fitting parameter taking into account the decrease in charge carrier concentration at the drain side [5]. The resistances are estimated as $R_s=R_c/2$, where R_c is total contact resistance, $R_i=1/(3g_m)$, $R_g=R_{\text{sh}}W_g/(3L_g)$ and $R_{\text{sh}}=0.08 \Omega$ is the gate electrode sheet resistance [2,6]. We assume that at low fields the Coulomb scattering dominates [7,8]. This allows us to find the R_c , low-field mobility (μ_0) and residual carrier concentration (n_0) as parameters via fitting the GFET transfer characteristics by the semi-empirical drain resistance (R_{ds}) model [2,9]

$$R_{\text{ds}} = R_c + \frac{L_g}{W_g} \frac{1}{e\mu_0 n}, \quad (2)$$

where $n = \left[n_0^2 + \left((V_{\text{gs}} + V_{\text{Dir}}) \frac{C_{\text{ox}}}{e} \right)^2 \right]^{1/2}$ is the carrier concentration, e is the elementary charge, V_{gs} and V_{Dir} are the gate-source and Dirac voltages, respectively. The intrinsic transconductance is calculated as [2,6]

$$g_m = \frac{v \cdot (C_{gs} + C_{gd})}{L_g}, \quad (3)$$

where v is the effective velocity of the charge carriers. It was shown that at the intrinsic drain field $E_{int} = (V_{ds} - I_{ds} R_c) / L_g$, where I_{ds} is the drain-source current, above approx. $1 \text{ V}/\mu\text{m}$ the velocity of the charge carriers in graphene tends to saturate and can be expressed as [3,10]

$$v = \frac{\mu_0 E_{int}}{\left[1 + \left(\mu_0 E_{int} / v_{sat}\right)^\gamma\right]^{\frac{1}{\gamma}}}, \quad (4)$$

where $\gamma=3$ is the fitting parameter for the v dependence on E_{int} found via delay time analysis [10]. We apply the model, which assumes that the saturation velocity is limited by inelastic emission of optical phonons (OPs) and can be approximated as [3,10]

$$v_{sat} = \frac{2 \omega_{OP}}{\pi \sqrt{m}} \sqrt{1 - \frac{\omega_{OP}^2}{4 \pi m v_F^2} \frac{1}{N_{OP} + 1}}, \quad (5)$$

where $\hbar \omega_{OP}$ is the OP energy, the $N_{OP} = 1 / [\exp(\hbar \omega_{OP} / k_B T) - 1]$ is the phonon occupation, $v_F \approx 10^8 \text{ cm/s}$ is the Fermi velocity and k_B is the Boltzmann constant. We ignore the self-heating effects and assume that the temperature $T=295 \text{ K}$. Previously we showed, using delay time analysis, that the effective saturation velocity in our GFETs is defined by the combination of the SiO_2 surface OPs and the graphene zone-edge OPs with $\hbar \omega_{OP} = 55 \text{ meV}$ and 200 meV , respectively [10]. The lines in Fig. 1 represent calculations using the Eqs. (1)-(5). The upper and lower dotted lines correspond to parameters of the GFETs with highest measured f_{max} (circle) and our previously published GFET (open square), respectively [2,10]. As it can be seen, there is a good agreement with experiments, which validates the used method of simulations combining the models of the drain resistance, carrier velocity and saturation velocity.

Analysis using Eqs. (1)-(5) indicates that f_{max} of the GFETs is limited, mainly, by the relatively high differential drain conductivity, which is caused by the zero energy bandgap in the monolayer graphene [1]. Fig. 2 shows the drain current density $j_{ds} = I_{ds} / W_g$ and corresponding differential drain conductivity $g_{ds-diff} = \partial j_{ds} / \partial E_{int}$ versus E_{int} of the GFET, with $L_g = 500 \text{ nm}$ and $W_g = 30 \mu\text{m}$, revealing highest measured $f_{max} = 37 \text{ GHz}$. It can be seen, that at $E_{int} \approx 1.7 \text{ V}/\mu\text{m}$, corresponding to the highest f_{max} , $g_{ds-diff} \approx 0.3 \text{ mS}$. For demonstration of the limiting effect of the drain conductance, the solid line in Fig. 1 shows the f_{max} , simulated using Eqs. (1)-(5) and the same GFET parameters, but assuming $g_{ds-diff} = 0.01 \text{ mS}$, which is typical for the Si MOSFETs [4]. It can be seen that f_{max} can be up to 300 GHz at $L_g = 200 \text{ nm}$. Approaches of decreasing g_{ds} via inducing a bandgap in graphene are, apparently, not promising because of simultaneous reduction in the carrier mobility and, hence, high-field velocity [1]. Our analysis indicates that a more favorable way is a selection of the adjacent dielectric materials with optical phonon energy higher than that of the SiO_2 . This will increase the saturation velocity limited by the remote phonon scattering [3,10]. The dashed and dash-dotted lines in Fig. 1 represent f_{max} , simulated using Eqs. (1)-(5) and the same GFET parameters, including $g_{ds-diff} \approx 0.3 \text{ mS}$, but with graphene encapsulated by Al_2O_3 and hexagonal boron nitride (hBN)

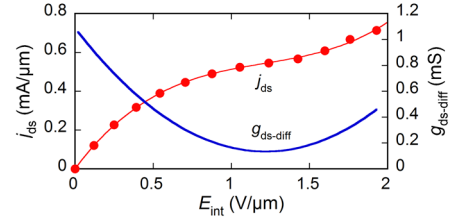


Fig. 2. Drain current density (j_{ds}) and differential drain conductivity ($g_{ds-diff}$) versus intrinsic drain field (E_{int}) of a GFET with $L_g=500 \text{ nm}$ and $W_g=30 \mu\text{m}$.

layers, respectively. The Al_2O_3 and hBN optical phonon energy are 87 and 100 meV , respectively, resulting in corresponding saturation velocity of approx. $3 \cdot 10^7$ and $5 \cdot 10^7 \text{ cm/s}$ [10]. It can be seen that the f_{max} of the Al_2O_3 and hBN encapsulated GFETs can be approx. 120 and 180 GHz , respectively, at $L_g=200 \text{ nm}$.

III. SUMMARY

In this work, we analyzed performance of the GFETs with high extrinsic $f_{max}=37 \text{ GHz}$, at $L_g=500 \text{ nm}$, using method of simulations combining the models of the drain resistance, carrier velocity and saturation velocity. It is shown, that the f_{max} is limited, mainly, by the relatively high differential drain conductivity of 0.3 mS , which is approx. 30 times higher than that typical for the Si MOSFETs. A promising approach of further development of the GFETs, suitable for the mm-wave amplifiers, is a selection of the adjacent dielectric materials with optical phonon energy higher than that of the SiO_2 , resulting in higher saturation velocity. According to the analysis, f_{max} of the Al_2O_3 and hBN encapsulated GFETs can be up to 120 GHz and 180 GHz , respectively, at $L_g=200 \text{ nm}$.

This work received funding in part from the European Union's Horizon 2020 research and innovation programme Graphene Flagship under grant agreement No 785219 (GrapheneCore2) and in part by the Swedish Research Council under grant No 2017-04504.

REFERENCES

- [1] F. Schwierz, "Graphene Transistors: Status, Prospects, and Problems," *Proceedings of the IEEE*, vol. 101, no. 7, pp. 1567-1584, July, 2013.
- [2] M. Bonmann, M. Asad, X. Yang, A. Generalov, A. Vorobiev, L. Banszerus, C. Stampfer, M. Otto, D. Neumaier and J. Stake, "Graphene Field-Effect Transistors With High Extrinsic f_t and f_{max} ," *IEEE Electron Device Lett.*, vol. 40, no. 1, pp. 131-134, January, 2019.
- [3] V. E. Dorgan, M.-H. Bae, and E. Pop, "Mobility and saturation velocity in graphene on SiO_2 ," *Appl. Phys. Lett.* vol. 97, pp. 082112-3, 2010.
- [4] R. A. Johnson, P. R. de la Houssaye, C. E. Chang, P.-F. Chen, M. E. Wood, G. A. Garcia, I. Lagnado, and P. M. Asbeck, "Advanced thin-film silicon-on-sapphire technology: Microwave circuit applications," *IEEE Trans. Electron Devices*, vol. 45, no. 5, pp. 1047-1054, May, 1998.
- [5] I. Meric, C. R. Dean, S.-J. Han, L. Wang, K. A. Jenkins, J. Hone, and K. L. Shepard, "High-frequency performance of graphene field effect transistors with saturating IV-characteristics," in *IEDM Tech. Dig.*, Washington, DC, USA, pp. 2.1.1-2.1.4, December, 2011.
- [6] S. M. Sze and K. K. Ng, *Physics of Semiconductor Devices*. Hoboken, NJ, USA: Wiley, 2007.
- [7] S. Adam, E. H. Hwang, V. M. Galitski, and S. Das Sarma, "A self-consistent theory for graphene transport," *Proc. Natl. Acad. Sci. U.S.A.*, vol. 104, no. 47, pp. 18392-18397, November, 2007.
- [8] F. Giannazzo, S. Sonde, R. L. Nigro, E. Rimini, and V. Raineri, "Mapping the density of scattering centers limiting the electron mean free path in graphene," *Nano Lett.*, vol. 11, pp. 4612-4618, October, 2011.
- [9] S. Kim, J. Nah, I. Jo, D. Shahrjerdi, L. Colombo, Z. Yao, E. Tutuc, and S. K. Banerjee, "Realization of a high mobility dual-gated graphene field-effect transistor with Al_2O_3 dielectric," *Appl. Phys. Lett.*, vol. 94, no. 6, pp. 062107-3, February, 2009.
- [10] M. Bonmann, A. Vorobiev, M. A. Andersson, and J. Stake, "Charge carrier velocity in graphene field-effect transistors," *Appl. Phys. Lett.*, vol. 111, no. 23, p. 233505-5, December, 2017.